

## CELL MECHANICS

## Two regimes, maybe three?

We have begun to understand the physical determinants of cell rheology and their relevance to biological functions. Experiments performed on freshly excised cells offer a new perspective in which soft-glass rheology and prestress seem to play central roles.

## DIMITRIJE STAMENOVIĆ

is in the Department of Biomedical Engineering, Boston University, 44 Cummings Street, Boston, Massachusetts 02215, USA.

e-mail: dimitrij@bu.edu

The ability of cells to alter their shape in response to mechanical stresses is essential for maintaining life. Certain fundamental functions, such as crawling, spreading and invading, require cells to become highly malleable. However, cells have to maintain their structural integrity under mechanical stress, and in order to do so they must behave like an elastic solid. The apparently ambivalent mechanical behaviour makes the study of cell rheology (the relationship between deformation and applied stress) particularly challenging. On page 636 of this issue, Deng and colleagues managed to reconcile the different mechanical responses of cells by studying, over a wide range of timescales, the microrheology of the cytoskeleton (CSK), the filamentous protein network that constitutes the scaffold of cells, and interpreting the results borrowing concepts from condensed-matter physics<sup>1</sup>.

The mechanical responses of cells are determined by the intrinsic mechanical properties of the CSK material, its architecture, and the stress-induced changes in biochemistry that modify the CSK structure. Many *in vitro* experiments on reconstituted actin (the major protein constituent of the CSK) gels suggest that the CSK must behave like a semiflexible polymer. In other words, over short times actin gels are viscoelastic, that is, they exhibit time–frequency dependence of their material moduli, but over long timescales they are elastic and their behaviour is time-independent<sup>2</sup>. Deng and colleagues probe the microrheology of excised smooth muscle cells by monitoring the displacement of ferrimagnetic beads attached to the cell surface and connected to the CSK through receptors that span the cell's membrane. Their results confirm that indeed the cell behaves like an actin gel, but only at small timescales!

A crucial element in this study is that the authors used freshly excised cells, which are one step closer to the cells *in situ*, whereas in previous studies on cultured cells the actin gel-like behaviour was not observed. Deng *et al.* argue that this reflects the

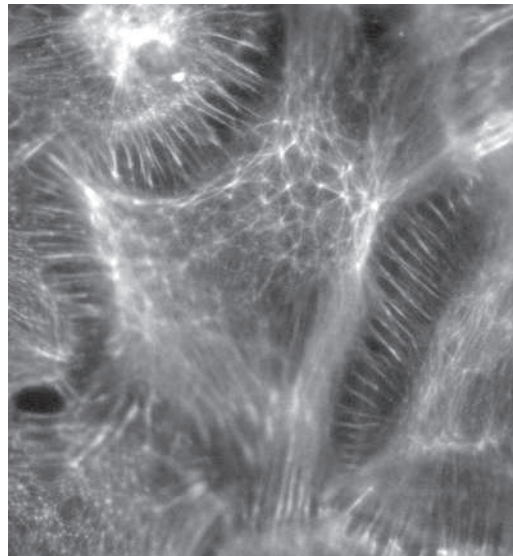


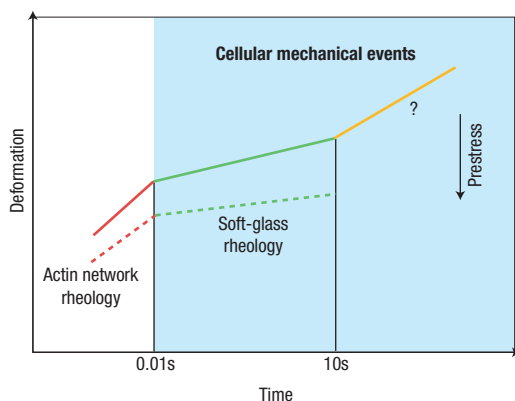
**Figure 1** The cytoskeletal actin network of mouse embryonic fibroblasts. The cells are stained with Alexa488-phalloidin to visualize filamentous actin. Courtesy of Julia Sero and Donald E. Ingber.

difference in the cytoskeletal organization between fresh and cultured smooth muscle cells<sup>1</sup>.

A number of microrheological studies on a variety of cell types indicate a similar type of mechanical response. A simple relationship, known as power law, has been found to describe how cells deform with time under a constant or an oscillatory mechanical stress. It suggests that under an applied stress, cells deform continuously and that this process is timescale invariant, that is, it does not depend on loading frequency<sup>3–5</sup>. This behaviour is more similar to soft glasses — fluid-like systems such as slurries or foams — and is well described by the theory of soft-glass rheology (SGR)<sup>3–5</sup>. Soft glasses are characterized by structural disorder; under a load, they undergo structural rearrangements in a never-ending search for order. On the macroscale, this results in a system that slowly deforms over a wide range of timescales. Although the physical basis of SGR in living cells is not yet fully understood, circumstantial evidence justifies its application<sup>5</sup>.

The work of Deng and colleagues unifies actin network dynamics and soft-glass dynamics in cell rheology. They show that the dynamic modulus of the cell scales with the frequency of

**Figure 2** What is relevant in cell rheology? A log–log plot of the creep response — a time course of cell deformation produced by a constant applied stress — summarizes the current understanding of cell rheology. The creep response is characterized by three regimes: an initial fast creep ( $\sim 0\text{--}0.01$  s) governed by the viscoelastic behaviour of the semi-flexible actin network (scales with the power-law exponent  $\alpha = 0.75$  indicated by the red segment)<sup>1,2</sup>; a very slow creep ( $\sim 0.01\text{--}10$  s) governed by the SGR dynamics ( $\alpha \approx 0.05\text{--}0.35$ , indicated by the green segment)<sup>1,3–5</sup>, and an intermediate slow creep (above  $\sim 10$  s, indicated by the yellow segment) governed by mechanisms that are still unknown ( $\alpha \approx 0.5$ )<sup>6,7</sup>. The slope of each of the segments is indicative of the corresponding  $\alpha$ . An increase in prestress (direction of the increase indicated by the arrow) causes a decrease in deformation (that is, an increase in stiffness) and a decrease in  $\alpha$ , as indicated by the dashed lines<sup>1,3,4,9</sup>. Integrated mechanical events of the cell (spreading, crawling, contracting, reorienting, invading and so on) are set within timescales that correspond to the intermediate–slow time regimes.



the applied stress following two distinct regimes: at high frequency ( $>100$  Hz) it is in a fast regime that is consistent with the dynamics of actin networks, in which the modulus scales with frequency with a universal power-law exponent  $\alpha = 0.75$ ; at low frequency ( $<100$  Hz) it is in a slow regime that is consistent with SGR, in which the modulus scales with frequency with a much smaller exponent  $\alpha = 0.05$ . From a biological point of view, these findings are enlightening. They suggest that the fast dynamics of actin networks is of little relevance because its influence is important only over short timescales ( $<0.01$  s), whereas in cells most integrated mechanical events (spreading, crawling, contracting) are set within much longer timescales.

One lingering question remains though — whether the SGR regime also extends to longer timescales ( $>100$  s). This is important considering the much longer time course of a number of cellular mechanical events. Previous studies performed on cultured cells<sup>6,7</sup> show that under constant stress, the initial slow deformation rate increases sharply after  $10\text{--}100$  s, suggesting that mechanisms other than the SGR might govern cell dynamics at long timescales. A more complete picture of cell dynamics will be achieved when those mechanisms will be identified.

Another issue to consider is that the CSK of living cells is mechanically prestressed<sup>8</sup>. This prestress is generated by molecular motors that generate forces transmitted by the actin network and through adhesion plaques to the extracellular matrix that counterbalances these forces. Microrheological measurements on cells have shown that the power-law exponent  $\alpha$  decreases with increasing prestress<sup>9</sup>. Because  $\alpha$  is an index of deformability ( $\alpha = 0$  corresponds to an elastic solid, whereas  $\alpha = 1$  corresponds to a flowing liquid such as water), the fact that  $\alpha$  changes with prestress suggests that this regulates the transition between solid-like and fluid-like behaviour in cells. More-recent experiments on actin gels also show a similar dependence of  $\alpha$  on prestress<sup>10</sup>. However, this behaviour is interpreted as a direct effect of the materials properties of the actin gel<sup>10</sup>, whereas in cells its origin may be related to the architectural organization of the CSK<sup>8</sup>. This is an intriguing question because it implies that dynamic rheological processes within the CSK are regulated by the static mechanical stress it bears, a concept that has not been included in the present rheological models of the cell. A complete understanding of the cell's ability to deform and adapt demands a better understanding of mechanisms by which the prestress influences cell rheology. The results of Deng *et al.* hint at a rheological model where SGR and prestress play central roles.

#### REFERENCES

- Deng, L. *et al.* *Nature Mater.* **5**, 636–640 (2006).
- Gardel, M. L. *et al.* *Phys. Rev. Lett.* **93**, 188102 (2004).
- Lenormand, G. & Fredberg, J. J. *Biorheology* **43**, 1–30 (2006).
- Fabry, B. *et al.* *Phys. Rev. Lett.* **87**, 14802 (2001).
- Bursac, P. *et al.* *Nature Mater.* **4**, 558–561 (2005).
- Despart, N., Richert, A., Simeon, J. & Asnacios, A. *Biophys. J.* **88**, 2224–2233 (2005).
- Overby, D. R., Matthews, B. D., Alsberg, E. & Ingber, D. E. *Acta Biomater.* **1**, 295–303 (2005).
- Wang, N. *et al.* *Proc. Natl. Acad. Sci. USA* **98**, 7765–7770 (2001).
- Stamenović, D., Suki, B., Fabry, B., Wang, N. & Fredberg, J. J. *J. Appl. Physiol.* **96**, 1600–1605 (2004).
- Gardel, M. L. *et al.* *Phys. Rev. Lett.* **96**, 088102 (2006).



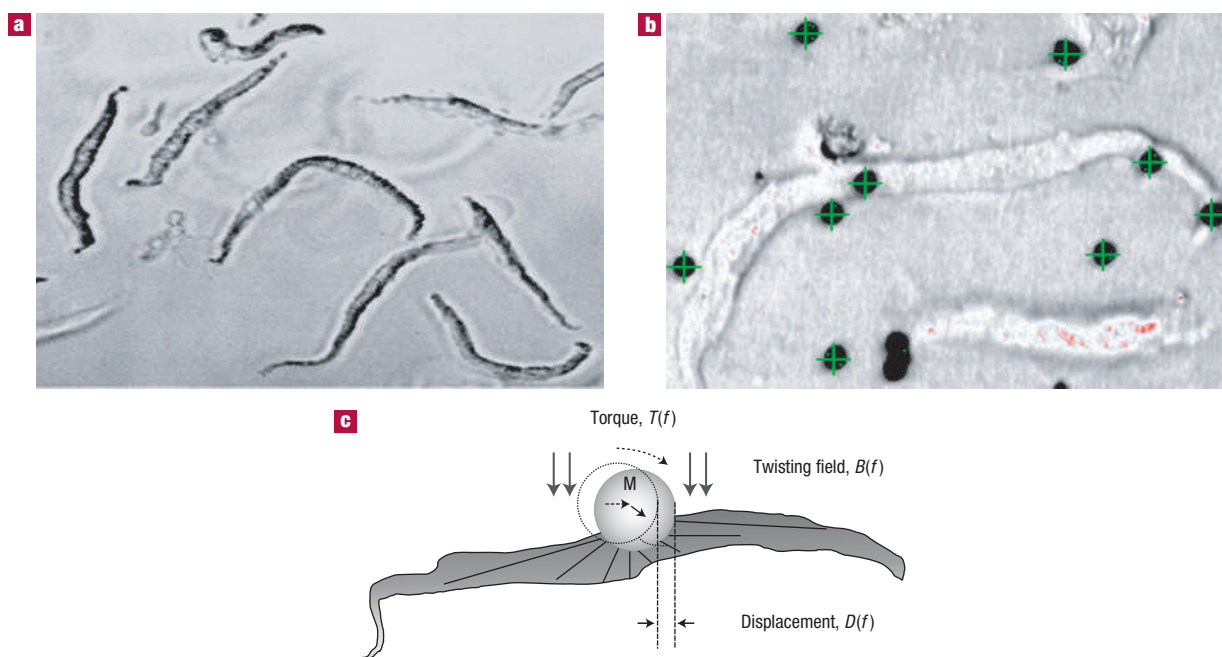


**Figure 1** Freshly isolated bovine trachea smooth muscle cells, with bound beads, and the twisting cytometry method. **a**, Photomicrograph of freshly isolated bovine trachea smooth muscle cells (typically 150 to 200 micrometres long) adhered to a poly-L-lysine substrate. Note the typical long worm-like appearance. 4–5 h after first settling on the substrate, healthy cells usually established firm attachment with various contact points. **b**, Bovine trachea smooth muscle cells with beads attached. RGD-coated ferrimagnetic beads were introduced and allowed to bind to the integrin receptors on the surface of the adherent cells (20 min). A charge-coupled device camera was used to identify each bead, which was then marked with a cross-hair determined by the centre position of its image. **c**, Schematic diagram of the magnetic twisting cytometry method in which the bead was oscillated at a frequency,  $f$ , from 0.09 to 1,000 Hz by a torque,  $T$ , caused by a sinusoidal magnetic field,  $B$ , of 20 G magnitude at  $f$ . The resultant sinusoidal displacement,  $D$ , of the bead was measured from the recorded bead positions during the oscillation.

slowly with frequency at frequencies below 100 Hz, but much more rapidly at frequencies greater than 100 Hz (Fig. 3). Compared with the frequency dependence of  $G'$ , that of  $G''$  was smaller at lower frequencies but higher at higher frequencies.

On a cell-by-cell basis, we fitted these data in the complex plane (see the Methods section) to the relationship  $G^*(f) = A(if)^\alpha + B(if)^\beta$ .  $G'$  data were well represented by the best fit, but  $G''$  data at lower frequencies fell systematically above and had weaker frequency dependence than indicated by the best fit (Fig. 3, solid lines); similar discrepancies have been reported in bronchial epithelial cells, macrophages and neutrophils<sup>24</sup>, and are a signature of soft glassy materials that are ageing<sup>25–28</sup>.

Although our technology is limited to frequencies below 1 kHz, our data were sufficient to resolve the exponents  $\alpha$  and  $\beta$  and put relatively narrow bounds on their values (see the additional comments on statistical tests in the Supplementary Information). Across the cell population ( $N = 64$ ), the distributions of  $\alpha$  and  $\beta$  were approximately normal (Fig. 4). The mean of  $\alpha$  was 0.05 (95% confidence interval 0.04–0.06) and was different from zero ( $p < 0.00001$ ); as described below, this implies that at low frequencies the system did not approach a hookean limit. The mean of  $\beta$  was 0.75, (95% confidence interval 0.69–0.79) and was different from unity ( $p < 0.00001$ ); as described below, this implies that at high frequencies the system did not approach a newtonian limit. Indeed, setting  $\beta$  to unity degraded the fit and adding a newtonian viscous term led to a result that was physically unrealizable (see the Supplementary Information).

Distinct values of  $\alpha$  and  $\beta$  imply that the rheology in these cells was characterized by two distinct regimes. In excess of 100 Hz, the complex modulus approached  $f^{0.75}$ , a scaling behaviour consistent

with that predicted by the theory of semiflexible polymers<sup>4,12,15,16</sup>. Such high-frequency dynamics have not been noted previously in the living cell although, in retrospect, a hint of such behaviour is evident in cells passaged in culture<sup>24</sup>. In contrast, at lower frequencies semiflexible-polymer dynamics became subdominant, with the complex modulus scaling as  $f^{0.05}$ . This exponent was non-universal, as shown below, and was systematically smaller than that observed in ASM cells passaged in culture, where, typically,  $0.1 < \alpha < 0.3$  (refs 8,17,24,29), but is comparable to that found in intact activated ASM strips (data not shown).

$G^*$  increased with contractile activation (KCl, 80 mM) and decreased with relaxation (dibutyryl cAMP, 1 mM) (Supplementary Information, Fig. S1). The exponent  $\beta$  was not influenced by relaxation, but decreased during contraction from 0.75 to 0.64 (95% confidence interval 0.57 to 0.71) (Supplementary Information Fig. S2, top), suggesting that contraction altered the qualitative nature of the high-frequency behaviour, whereas relaxation did not. Values of  $\beta$  smaller than 3/4 are consistent with behaviour observed in pre-stressed F-actin gels<sup>14</sup>. Indeed, pre-stress in cells<sup>17,30</sup> and in filamin-crosslinked gels<sup>20</sup> is known to be a major determinant of dynamics in the slow glassy regime, but the role of pre-stress in the fast regime could not be addressed in the experiments described here and remains a major open question. The exponent  $\alpha$  decreased slightly during cell contraction, but during cell relaxation it increased from 0.05 to 0.08 (95% confidence interval 0.06 to 0.09) (Supplementary Information, Fig. S2, bottom).

Why should material moduli at low frequencies scale with a weak non-universal exponent? When taken together with other observations, such behaviour has been taken as strong evidence

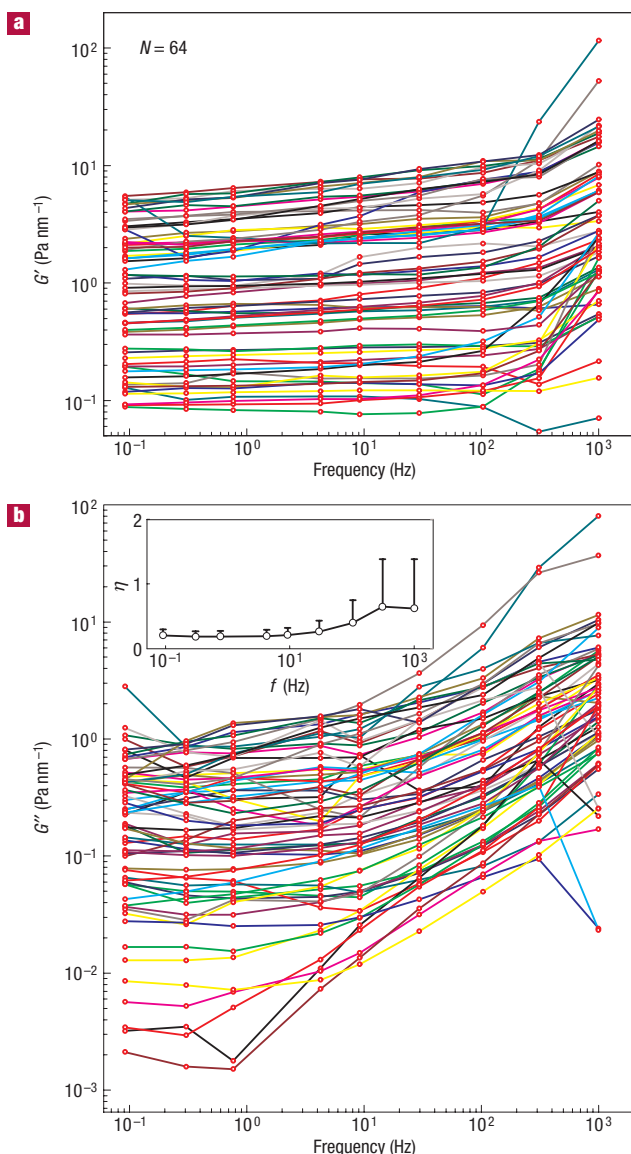


**Figure 2** Storage modulus ( $G'$ ) and loss modulus ( $G''$ ) as a function of frequency for all beads measured ( $N=64$ ). **a,b**,  $G'$  (**a**) and  $G''$  (**b**) varied broadly across beads, approximately log-normally. However, the hysteresivity or loss tangent  $\eta = G''/G'$  varied little across beads, and only weakly with frequency (inset, mean  $\pm$  standard deviation).

for non-equilibrium behaviour and, in particular, a glassy regime of CSK dynamics has been suggested<sup>8,9</sup>. The ability of a liquid to form a glass is related to slowly relaxing degrees of freedom which, under certain conditions, may persist out of equilibrium<sup>31</sup>. By the term 'slow', here we mean processes that decay more slowly than any exponential, such as logarithmic or weak power-law decay. In various inert glassy systems, slow degrees of freedom have been attributed to a variety of possibilities, including slow motions of polymer chains constrained by chemical crosslinks, entanglements or loops, slow turnover of covalent or non-covalent bonds connecting constituent structures to form a bond network, slow relaxation towards energetically favourable configurations, and slow structural rearrangements arising from crowding, caging, and jamming<sup>32–35</sup>. Despite this variety, traditional glassy systems share one feature in common: slow localized inelastic rearrangements,

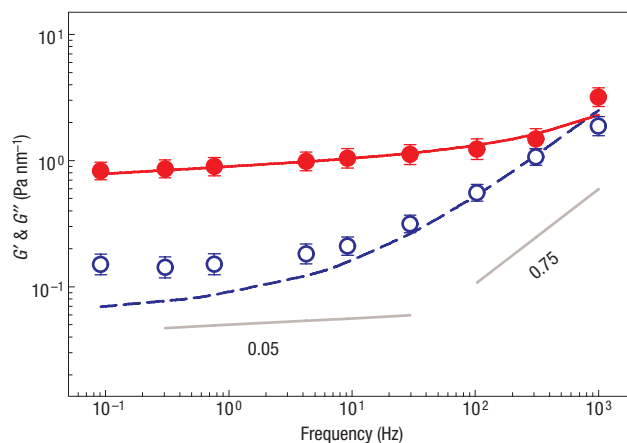


**Figure 3** Pooled data of  $G'$  (red, filled circles) and  $G''$  (blue, open circles) from all individual beads, together with the average two-term power-law fit (solid lines). The data presented are the geometric mean, and the corresponding error bars represent the geometric standard error defined as the standard error of the data set in logarithmic space. The solid lines represent the two-term power-law fit with geometric means of  $A$  and  $B$ , and arithmetic means of  $\alpha$  and  $\beta$ . This graph clearly demonstrates the two regimes of frequency dependence measured in the freshly isolated ASM cell. At lower frequencies, the moduli increased with frequency as a weak power law with exponent 0.05. At higher frequencies, the moduli increased as a stronger power law with exponent 0.75. The transition occurred at about 100 Hz. The straight grey lines denote slopes of 0.05 and 0.75.

and the applicability of such a point of view is justified by the universality of the phenomenology<sup>25,31</sup>. In the living cell, none of the above can be ruled out and, as we suggested previously, ATP-dependent rearrangements might modify CSK microconfigurations and thereby provide an alternate means of exploring new network configurations<sup>9</sup>. ATP hydrolysis can drive both conformational changes and polymerization/depolymerization cycles of CSK proteins, either or both of which could conceivably resolve constraints and drive structural rearrangements.

Consistent with that physical picture<sup>9,25,36</sup>, but in contrast with equation (1), the complex modulus of the ASM cell passaged in culture has been shown to go as<sup>8,24</sup>

$$G^*(f) \sim G_0 \Gamma(1-\alpha) \{i2\pi f / \Phi_0\}^\alpha, \quad (2)$$

where  $\Gamma()$  is the gamma function, and  $G_0$  and  $\Phi_0$  are scale factors for stiffness and frequency, respectively, and again we have suppressed a small newtonian viscosity.

We suggest that equations (1) and (2) describe the high-frequency [ $B(if)^{3/4}$ ] and low-frequency [ $A(if)^\alpha$ ] terms of the best fit, respectively. As regards low-frequency behaviour of the CSK<sup>8,18,19,24,29</sup> and equation (2), the non-universal exponent  $\alpha$  becomes a continuous measure of proximity of the CSK to solid-like ( $\alpha=0$ ;  $G''=0$ ) versus fluid-like ( $\alpha=1$ ;  $G'=0$ ) behaviours. In contrast, the observation of  $G^*$  approaching  $f^{3/4}$  at higher frequencies suggests the emergence of entropic dynamics associated with semiflexible polymers and in this report it is identified for the first time in living cells. Despite uncertainties in the values of the various factors in equation (1), values found in the literature yield a prefactor,  $B$ , that is within an order of magnitude of that which was observed experimentally; this correspondence represents independent evidence that the fast regime indeed arises from dynamics of semiflexible polymers.

Therefore, we conclude that in the living cell the dynamics of semiflexible polymers and soft glasses coexist, but each dominates

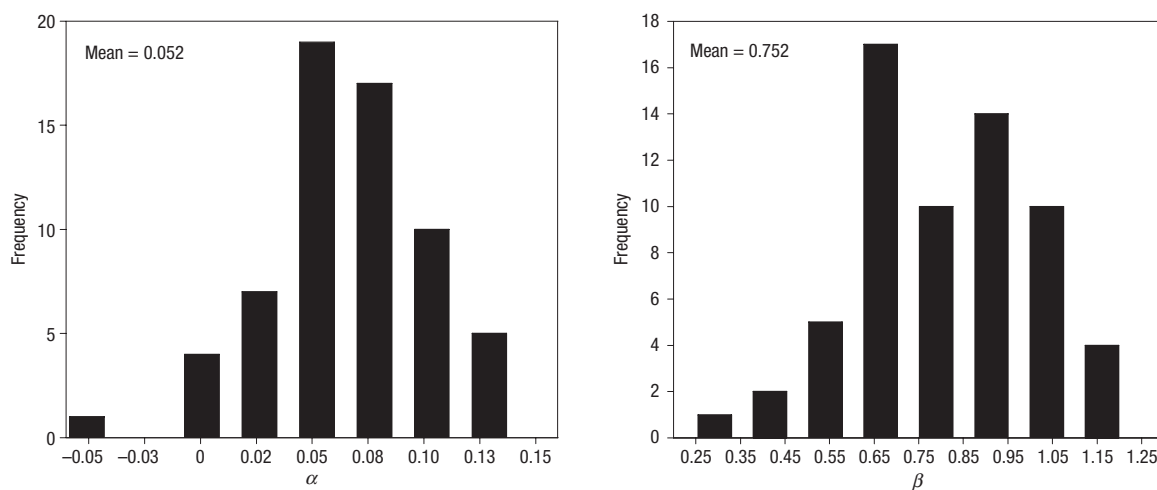


**Figure 4** Distributions of the two exponents,  $\alpha$  and  $\beta$ , that characterize the two distinct regimes of CSK dynamics. These were both approximately normal. The mean and standard deviation of  $\alpha$  were 0.05 and 0.036, respectively (95% confidence interval 0.04–0.06). The mean and standard deviation of  $\beta$  were 0.75 and 0.19 (95% confidence interval 0.69–0.79). A Student's *t*-test verified that  $\alpha$  was significantly different from zero ( $p < 0.00001$ ), and  $\beta$  was significantly different from unity ( $p < 0.00001$ ), but not different from 0.75 ( $p > 0.5$ ).

on different timescales. On shorter timescales (higher frequencies), there is insufficient time for inelastic structural rearrangements and, as such, relatively fast thermal fluctuations drive bending of semiflexible CSK filaments and determine material properties of the CSK. In this fast regime, as crosslink density increases, entropic contributions to the elasticity diminish relative to the enthalpic contributions<sup>14</sup>. However, on longer timescales (lower frequencies) slow inelastic rearrangements of the CSK prevail<sup>8,9</sup>, and the effects of thermally driven filament bending become subdominant. Such an interpretation implies sustained departure from thermodynamic equilibrium and is consistent with the finding that in the living ASM cell on longer timescales the generalized Stokes–Einstein relationship breaks down<sup>9</sup>.

It was not obvious *a priori* that entropic effects could be responsible for cell elasticity. The results presented here are the first evidence to suggest that they are. As these results resemble so clearly what is seen in simple reconstituted but crosslinked actin networks, they also strongly support the idea that the bead-twisting probe we used is most sensitive to the cytoskeletal actin network. All prior measurements in other cell systems show power-law responses with non-universal exponents in the range 0.1–0.3 (refs 8,17–19,24,29), and it was not clear from those measurements if a distinct high-frequency regime might exist. The results presented here show that such a regime does exist and that its exponent is 3/4.

As such, data reported here unify within the same cell these two distinct schools of thought, and suggest that the transition between regimes occurs on timescales of the order of  $10^{-2}$  s. Accordingly, these data set within the slow glassy regime timescales typical of integrated mechanical events of the cell such as spreading, crawling, contracting, and invading.

## METHODS

All chemical reagents, standard buffer solutions, and media were purchased from Sigma unless stated otherwise.

### PREPARATION OF INTACT LIVING CELLS

Single ASM cells were freshly isolated from bovine trachea by enzymatic digestion, which was adopted from a previously described method<sup>23</sup>. Briefly, a

bovine trachea was obtained from an abattoir and transported to the laboratory within 2 h of excision. Before use, the tissue was maintained at 4 °C in an oxygenated (95% O<sub>2</sub> and 5% CO<sub>2</sub>) buffer containing 1:1 Hank's balanced salt solution and Dulbecco's modified Eagle's medium, and 1,000 Unit ml<sup>-1</sup> of penicillin and streptomycin. Subsequently, in constantly oxygenated Krebs solution (120 mM NaCl, 5.9 mM KCl, 1.2 mM NaH<sub>2</sub>PO<sub>4</sub>, 25 mM NaHCO<sub>3</sub>, 11.5 mM dextrose, 1 mM CaCl<sub>2</sub>, and 1.4 mM MgCl<sub>2</sub>), 50 mg wet weight of ASM was dissected from the trachea and cut into 2 × 3 mm pieces. The tissue was then transferred into a siliconized, that is, coated with SigmaCote, flask containing an enzymatic digestion solution. The digestion solution consisted of 182 Unit ml<sup>-1</sup> Type 2 collagenase (Worthington), 3.0 Unit ml<sup>-1</sup> Grade II elastase (Roche Diagnostics), and 5,000 Unit ml<sup>-1</sup> Type II-S soybean trypsin inhibitor in a Ca<sup>2+</sup> and Mg<sup>2+</sup> free buffer consisting of 137 mM NaCl, 5.4 mM KCl, 5.6 mM dextrose, 4.2 mM NaHCO<sub>3</sub>, 0.42 mM Na<sub>2</sub>HPO<sub>4</sub>, 0.44 mM KH<sub>2</sub>PO<sub>4</sub>, and 0.075% bovine serum albumin. The tissue was incubated in this digestion solution in a shaking water bath (9.6 cycles min<sup>-1</sup>) at 34 °C and oxygenated atmosphere for 40 min. The dissociated cells were filtered through nylon gauze (526 μm mesh size) and rinsed with 10 ml of the Ca<sup>2+</sup> and Mg<sup>2+</sup> free buffer. More cells may be harvested by repeatedly incubating the remaining tissue in the digestion solution, but in a progressively reduced concentration of collagenase.

Dissociated cells were poured over glass coverslips or 96 wells coated with poly L-lysine and incubated for 40 min on ice. Cell viability was verified by KCl-induced contraction of sample cells in each batch of harvested cells.

Because these cells were adherent on a rigid substrate at the time of measurement, all contractions were isometric. Although we did not use traction microscopy to measure contractile stresses, as we have in our previous work<sup>17,30</sup>, these cells probably do maintain appreciable axial tension.

### MEASUREMENT OF THE DYNAMIC MODULUS

To probe the microrheology of CSK, ferrimagnetic beads (4.5 μm diameter) were coated with a synthetic peptide containing the Arg–Gly–Asp (RGD; Peptide 2000, Integra Life Sciences) sequence and allowed to adhere to the apical cell surface. These beads become tightly tethered to the F-actin CSK through transmembrane integrin receptors, mostly  $\alpha_5\beta_1$ ; these receptors bind to the RGD ligand in the extracellular domain and the focal adhesion and actin filaments in the intracellular domain<sup>1,8,24,29,37–39</sup> (Fig. 1b). We then measured the complex modulus as a function of frequency by applying an oscillatory magnetic field and measuring the resultant oscillatory bead motions with light microscopy<sup>24,37</sup> (Fig. 1c). When the oscillatory magnetic field of frequency  $f$  was applied to the bead, it resulted in an oscillatory torque  $\tilde{T}$ , where the tilde overbar denotes the Fourier domain. The induced lateral displacement of the

bead,  $\tilde{D}$ , was measured using a charge-coupled device camera attached to an inverted optical microscope (Leica Microsystems). The complex modulus is then simply

$$G^*(f) = \tilde{T} / \tilde{D}.$$

$G^*$  measured in this way has units of torque per unit bead volume per unit bead displacement, or Pa nm<sup>-1</sup>. This can be converted to familiar material moduli with the use of a length scale derived from a model of cell deformation<sup>40</sup>, but to avoid model-dependent assumptions here we report all data in primary measurement units of Pa nm<sup>-1</sup>.

#### DATA ANALYSIS AND FITTING

Denote the complex modulus of the  $n$ th bead at frequency  $f_m$  by  $G_n^*(f_m)$ . For each bead (that is, for each  $n$ ), the two-term power-law model,  $G^*(f) = A(if)^\alpha + B(if)^\beta$  was fitted to these data by minimizing  $\sum_{m=1}^M |\log G^*(f_m) - \log G_n^*(f_m)|^2$  with respect to the parameters  $A$ ,  $B$ ,  $\alpha$ ,  $\beta$ .  $M$  is the number of frequencies used, typically 9, spanning 0.1 Hz to 1 kHz in half log increments. The distributions of the parameters obtained from this bead-by-bead fit were examined statistically. R project, a freely available statistical software package ([www.r-project.org](http://www.r-project.org)), was used to fit the model to the data and for statistical analysis. One-way analysis of variance, and Student's  $t$ -test were used to examine the differences in the parameters when compared among multiple conditions or between two conditions, respectively. Differences with  $p < 0.05$  were considered statistically significant.

Received 17 February 2006; accepted 19 May 2006; published 9 July 2006.

#### References

- Chicurel, M. E., Chen, C. S. & Ingber, D. E. Cellular control lies in the balance of forces. *Curr. Opin. Cell Biol.* **10**, 232–239 (1998).
- Discher, D. E., Janmey, P. & Wang, Y. L. Tissue cells feel and respond to the stiffness of their substrate. *Science* **310**, 1139–1143 (2005).
- Janmey, P. A. & Weitz, D. A. Dealing with mechanics: mechanisms of force transduction in cells. *Trends Biochem. Sci.* **29**, 364–370 (2004).
- Gittes, F., Schnurr, B., Olmsted, P. D., MacKintosh, F. C. & Schmidt, C. F. Microscopic viscoelasticity: Shear moduli of soft materials determined from thermal fluctuations. *Phys. Rev. Lett.* **79**, 3286–3289 (1997).
- Morse, D. C. Viscoelasticity of concentrated isotropic solutions of semiflexible polymers. 2. Linear response. *Macromolecules* **31**, 7044–7067 (1998).
- Gardel, M. L., Valentine, M. T., Crocker, J. C., Bausch, A. R. & Weitz, D. A. Microrheology of entangled F-actin solutions. *Phys. Rev. Lett.* **91**, 158302 (2003).
- Gardel, M. L. *et al.* Elastic behavior of cross-linked and bundled actin networks. *Science* **304**, 1301–1305 (2004).
- Fabry, B. *et al.* Scaling the microrheology of living cells. *Phys. Rev. Lett.* **87**, 148102 (2001).
- Bursac, P. *et al.* Cytoskeletal remodelling and slow dynamics in the living cell. *Nature Mater.* **4**, 557–561 (2005).
- Kas, J., Strey, H. & Sackmann, E. Direct imaging of reptation for semiflexible actin filaments. *Nature* **368**, 226–229 (1994).
- MacKintosh, F. C., Kas, J. & Janmey, P. A. Elasticity of semiflexible biopolymer networks. *Phys. Rev. Lett.* **75**, 4425–4428 (1995).
- Gittes, F. & MacKintosh, F. C. Dynamic shear modulus of a semiflexible polymer network. *Phys. Rev. E* **58**, R1241–R1244 (1998).
- Gisler, T. & Weitz, D. A. Scaling of the microrheology of semidilute F-actin solutions. *Phys. Rev. Lett.* **82**, 1606–1609 (1999).
- Gardel, M. L. *et al.* Scaling of F-actin network rheology to probe single filament elasticity and dynamics. *Phys. Rev. Lett.* **93**, 188102 (2004).

- Morse, D. C. Viscoelasticity of tightly entangled solutions of semiflexible polymers. *Phys. Rev. E* **58**, R1237–R1240 (1998).
- Morse, D. C. Viscoelasticity of concentrated isotropic solutions of semiflexible polymers. 1. Model and stress tensor. *Macromolecules* **31**, 7030–7043 (1998).
- Stamenovic, D., Suki, B., Fabry, B., Wang, N. & Fredberg, J. J. Rheology of airway smooth muscle cells is associated with cytoskeletal contractile stress. *J. Appl. Physiol.* **96**, 1600–1605 (2004).
- Alcaraz, J. *et al.* Microrheology of human lung epithelial cells measured by atomic force microscopy. *Biophys. J.* **84**, 2071–2079 (2003).
- Desprat, N., Richert, A., Simeon, J. & Asnacios, A. Creep function of a single living cell. *Biophys. J.* **88**, 2224–2233 (2005).
- Gardel, M. L. *et al.* Prestressed F-actin networks cross-linked by hinged filaments replicate mechanical properties of cells. *Proc. Natl Acad. Sci. USA* **103**, 1762–1767 (2006).
- Draeger, A., Stelzer, E., Herzog, M. & Small, J. Unique geometry of actin-membrane anchorage sites in avian gizzard smooth muscle cells. *J. Cell Sci.* **94**, 703–711 (1989).
- Bagby, R. M., Young, A. M., Dotson, R. S., Fisher, B. A. & McKinnon, K. Contraction of single smooth muscle cells from *Bufo marinus* stomach. *Nature* **234**, 351–352 (1971).
- DeFoe, T. T. & Morgan, K. G. Responses of enzymatically isolated mammalian vascular smooth muscle cells to pharmacological and electrical stimuli. *Pflügers Arch.* **404**, 100–102 (1985).
- Fabry, B. *et al.* Time scale and other invariants of integrative mechanical behavior in living cells. *Phys. Rev. E* **68**, 041914 (2003).
- Sollich, P., Lequeux, F., Hebraud, P. & Cates, M. E. Rheology of soft glassy materials. *Phys. Rev. Lett.* **78**, 2020–2023 (1997).
- Cates, M. E. & Sollich, P. in *Foams and Emulsions* (eds Sadoc, J. F. & Rivier, N.) 207–236 (Kluwer Academic, Dordrecht, 1999).
- Mason, T. G., Gisler, T., Kroy, K., Frey, E. & Weitz, D. A. Rheology of F-actin solutions determined from thermally driven tracer motion. *J. Rheol.* **44**, 917–928 (2000).
- Gopal, A. D. & Durian, D. J. Relaxing in foam. *Phys. Rev. Lett.* **91**, 188303 (2003).
- Puig-de-Morales, M. *et al.* Cytoskeletal mechanics in adherent human airway smooth muscle cells: probe specificity and scaling of protein-protein dynamics. *Am. J. Physiol. Cell Physiol.* **287**, C643–C654 (2004).
- Wang, N. *et al.* Cell prestress. 1. Stiffness and prestress are closely associated in adherent contractile cells. *Am. J. Physiol. Cell Physiol.* **282**, C606–C616 (2002).
- Bulatov, V. V. & Argon, A. S. A stochastic model for continuum elastoplastic behavior. 2. A study of the glass-transition and structural relaxation. *Modelling Simul. Mater. Sci. Eng.* **2**, 185–202 (1994).
- Weeks, E. R., Crocker, J. C., Levitt, A. C., Schofield, A. & Weitz, D. A. Three-dimensional direct imaging of structural relaxation near the colloidal glass transition. *Science* **287**, 627–631 (2000).
- Mazurin, O. V. Theory of glass-transition—chemical-equilibria approach. *J. Non-Cryst. Solids* **129**, 259–265 (1991).
- Kovacs, A. J., Aklonis, J. J., Hutchinson, J. M. & Ramos, A. R. Isobaric volume and enthalpy recovery of glasses. 2. Transparent multi-parameter theory. *J. Polym. Sci. Polym. Phys.* **17**, 1097–1162 (1979).
- Chen, H. S. & Turnbull, D. Evidence of a glass-liquid transition in a gold-germanium-silicon alloy. *J. Chem. Phys.* **48**, 2560–2571 (1968).
- Sollich, P. Rheological constitutive equation for a model of soft glassy materials. *Phys. Rev. E* **58**, 738–759 (1998).
- Wang, N., Butler, J. P. & Ingber, D. E. Mechanotransduction across the cell surface and through the cytoskeleton. *Science* **260**, 1124–1127 (1993).
- Deng, L., Fairbank, N. J., Fabry, B., Smith, P. G. & Maksym, G. N. Localized mechanical stress induces time-dependent actin cytoskeletal remodeling and stiffening in cultured airway smooth muscle cells. *Am. J. Physiol. Cell Physiol.* **287**, C440–C448 (2004).
- Choquet, D., Felsenfeld, D. P. & Sheetz, M. P. Extracellular matrix rigidity causes strengthening of integrin-cytoskeleton linkages. *Cell* **88**, 39–48 (1997).
- Mijailovich, S. M., Kojic, M., Zivkovic, M., Fabry, B. & Fredberg, J. J. A finite element model of cell deformation during magnetic bead twisting. *J. Appl. Physiol.* **93**, 1429–1436 (2002).

#### Acknowledgements

The authors would like to thank C. Gallant for her assistance in the adaptation of the cell isolation method. X.T. is supported by a postdoctoral fellowship from the Spanish Ministerio de Educación y Ciencia. This study was financially supported by NIH HL65960, HL33009 and HL31704. Correspondence and requests for materials should be addressed to L.D. Supplementary Information accompanies this paper on [www.nature.com/naturematerials](http://www.nature.com/naturematerials).

#### Competing financial interests

The authors declare that they have no competing financial interests.

Reprints and permission information is available online at <http://npg.nature.com/reprintsandpermissions/>